ACI 83

# AN OPTIMAL OUTPUT FEEDBACK SOLUTION TO THE STRIP SHAPE MULTIVARIABLE CONTROL PROBLEM

J. V. Ringwood and M.J. Grimble

Industrial Control Unit
Department of Electronic & Electrical Engineering
University of Strathclyde
George Street, Glasgow, Scotland

ABSTRACT

The design of shape control systems for producing flat metal strip products is discussed. Static and dynamic models for a Sendzimir mill are described briefly. Optimal dynamic output feedback solutions are presented for the shape control system design. The optimal control solutions provide guidance on the best structure to be used for shape control. It is shown that by judicious choice of the performance criterion weighting matrices particularly simple controllers may be derived; dimension reduction by parameterisation is also shown to result in a simplification to the controller structure.

The effect of nonlinearities in the actuators is discussed, a linear approximation being used for design purposes.

A variety of simulation results are presented showing the transient response and the shape control performance of the multivariable system. The effect of mismatch is also demonstrated, that is, using the controller for a mill schedule other than the one for which it was designed.

## 1. INTRODUCTION

There are now well established techniques for the design of gauge control systems in metal strip rolling mills (Bryant 1973[1]). Current interest is centred upon the control of the internal stresses in rolled strip. This is referred to as shape control which is an unfortunate misnomer that often causes confusion. Strip is said to have good shape if it is free of internal stresses after it has been removed from mill and cut into sections. Sections of strip with good shape will lie flat on a flat surface. Whilst strip is being rolled it is under very high tensions and shape defects are often not apparent to the eye. Such shape defects are often referred to as latent shape. A direct measurement of flatness (as the deviation of a released sheet from a plane) is not possible whilst the material is being rolled. Reliable shape measuring devices have become available only during the last decade (Grimble 1975[2]). These devices are mainly used to provide a display of strip shape but have recently been used in closed-loop shape control systems, Sivilotti et al, 1973[3].

Bad shape is a consequence of a transverse variation of the rolling elongation. This can occur during both the hot rolling and subsequent cold rolling stages. Assume that the gauge profile entering the mill stand is of a uniform thickness and that the work rolls in the stand are deformed so that the strip exiting from the stand is thicker in the central region than at the edges. In the absence of lateral spread any differential reduction will tend to produce differential elongations in adjacent longitudinal elements of the strip (Sabatini and Yeomans, 1968[4]). Thus, due to the mass flow relationship, the strip will tend to be longer at the edges than it is in the central region. Since the strip is one homogeneous mass such differential elongations cannot occur and internal stresses result. If these differential stresses are sufficiently large, long edges to the strip will appear as a visible wavy edge (manifest shape). This can occur even when rolling materials such as stainless steel, where very high tensions are involved. From the viewpoint of the marketability of strip steel, shape is much more important than its accuracy of thickness across the strip.

It is sometimes possible to correct for bad shape stemming from the hot rolling process in the cold rolling stage. This paper is concerned with the cold rolling process only, with particular application to a Sendzimir Twenty-High Roll Cold Rolling Mill. The shape control problem for such a mill is a complex multivariable design problem. Using static and dynamic mill models a solution is determined by the application of optimal control theory. The controller currently being implemented on the mill was designed (Grimble and Fotakis, 1982[5]), by a related but nonoptimal approach. This present study assesses the advantages that might be gained by using the more complicated optimal controller.

## 2. SENDZIMIR MILL MODEL

A view of the physical layout of the mill is as shown in Fig.1.

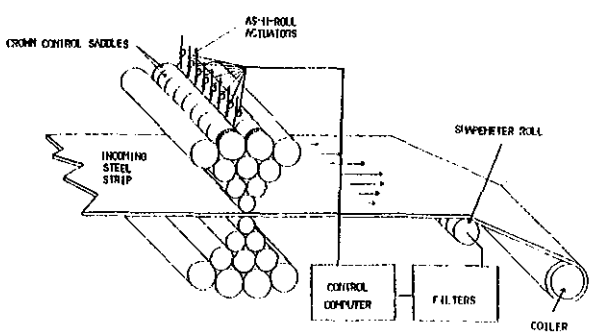


Figure 1: Physical Layout of Mill

This can be represented in the block diagram form as in Fig.2.

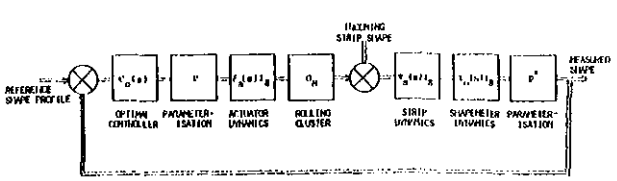


Figure 2: System Block Diagram

It is assumed that there are no dynamics associated with the rolling cluster itself (represented by $G_M$ in the block diagram) and so it is possible to divide the mill model up into its static and dynamic parts. This is necessary for computation and simulation purposes.

2.1 Static Model

The static model generates, for a specific set of rolling parameters (strip width, gauge, tension, etc.), an 8×8 matrix of constant coefficients which relates the shape profile at the roll gap to the movement of the As-U-Roll actuators. This model has been developed by Gunawardene et al (1980[5]). It allows for the bending and flattening of the rolls in the mill cluster and for the plastic deformation of the strip in the roll-gap.

It is convenient to calculate the shape at eight equally spaced points across the strip as this results in a square matrix, there being eight As-U-Roll actuators equally spaced across the top of the mill stand.

Due to the mill construction, the mill matrix has some special properties:

(a) Row sums are zero:

$$\sum_{j=1}^{8} g_{ij} = 0 \qquad i=1,\ldots,8 \tag{1}$$

where $g_{ij}$ are the elements of the mill matrix, $G_M$. This follows since a constant small equal change in each of the actuator racks produces a corresponding change in the mean tension stress but no change in shape; shape being defined as the deviation from the mean tension stress.

(b) Column sums are zero:

$$\sum_{i=1}^{8} g_{ij} = 0 \qquad j=1,\ldots,8 \tag{2}$$

This follows since shape represents the deviaiton from the mean tension stress and thus the mean shape is zero. A typical mill matrix is defined as:

$$\begin{bmatrix} 5.09 & 6.34 & 0.26 & -2.48 & -2.80 & -2.38 & -1.98 & -2.02 \\ 1.00 & 3.34 & 3.13 & 0.255 & -2.05 & -2.61 & -2.22 & -2.24 \\ -0.89 & 0.48 & 3.37 & 2.50 & -0.51 & -2.36 & -2.43 & -2.42 \\ -1.34 & -1.48 & 1.38 & 3.30 & 1.94 & -0.89 & -2.33 & -2.34 \\ -1.17 & -2.25 & -0.98 & 1.75 & 3.35 & 1.52 & -1.48 & -1.56 \\ -1.00 & -2.38 & -2.32 & -0.62 & 2.31 & 3.36 & 0.72 & 0.63 \\ -0.94 & -2.29 & -2.69 & -2.21 & -0.16 & 2.83 & 3.68 & 3.78 \\ -0.85 & -1.87 & -2.08 & -2.37 & -1.96 & 0.59 & 5.93 & 6.06 \end{bmatrix}$$

Note that the row and column sum properties do no hold exactly for this matrix. This is due to numerical computational inaccuracies and the fact that the mill is nonlinear.

Due to these properties, the mill matrix is singular but may be made nonsingular by constant input-output transformations which reduce the effective number of inputs and outputs (see following section). Thus without loss of generality $G_M$ (or its transform) will be assumed invertible. This is a property which is exploited in later sections.

2.2 Dynamic Model

The dynamic model contains all the blocks shown in Fig.2 and uses the mill matrices generated by the static model to obtain the shape at the roll-gap determined by the actuator positions. Each individual part will now be described briefly.

2.2.1 Reference shape profile. This is input as a set of four parameters which describe the desired shape profile. Generally a flat shape profile is desirable.

2.2.2 Input/output transformations. It is convenient to parameterise the shape profile so that the effective system outputs are the coefficients in a polynomial. Assuming the shape profile may be represented by a quartic equation, the shape at any point on the strip is given by:

$$S(z,t) = y_4(t)z^4 + y_3(t)z^3 + y_2(t)z^2 + y_1(t)z \tag{3}$$

where z is the distance across the strip, measured from its centre and normalised so that $z\in[-1,1]$. The relationship between the shape outputs and the parameter values may be represented by:

$$\underline{y}(t) = P\underline{y}_p(t) + \underline{e}(t) \tag{4}$$

where e(t) is an error term. The least squares estimate follows as:

$$\underline{y}_p(t) = P^* y(t) \tag{5}$$

where

$$P^* = (P^T P)^{-1} P^T \tag{6}$$

Note that there is no constant term in (3) as it is not required to control the mean stress across the strip.

The system may be made square to produce a new 4×4 effective $G_M$ matrix ($G_M$) by using an 8×4 input transformation N. This transformation might be chosen so that $G_M = P^* G_M N$ is a diagonal matrix. However, this does not allow the range of settings on the As-U-Roll shape actuators to be limited. If, alternatively, the transformation (based now upon orthonormal functions) is taken as P then $G_M = P^T G_M P$ and $\underline{u}_a(t) = P\underline{u}(t)$ and the settings on these actuators are limited to polynomial forms which is desirable from mechanical considerations.

The following parameterisation matrix will be used in the design:

$$\begin{bmatrix} 1.0 & 0.71 & 0.42 & 0.14 & -0.14 & -0.42 & -0.71 & -1.0 \\ 1.0 & 0.02 & -0.63 & -0.95 & -0.95 & -0.63 & 0.02 & 1.0 \\ 1.0 & -0.68 & -0.97 & -0.41 & 0.41 & 0.97 & 0.68 & -1.0 \\ 1.0 & -0.99 & -0.19 & 0.84 & 0.84 & -0.19 & -0.99 & 1.0 \end{bmatrix}$$

2.2.3 As-U-Roll actuators. Each actuator can be represented by a SISO system as shown in Fig.3.

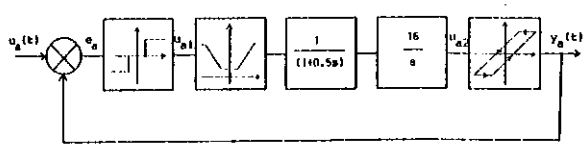


Figure 3: Actuator Block Diagram

It is seen that each actuator loop contains three nonlinear blocks. For the purposes of controller design it will be assumed that the actuator transfer function

$$y_a(t) = f_a(u_a, u_{a1}, u_{a2}, e_a, t) \tag{7}$$

may be represented by the linear second-order transfer function

$$y_a(t) = \frac{1}{(1+0.25s)(1+0.53s)}\, u_a(t) \tag{8}$$

This transfer function was derived using a combination of frequency response and time response comparison techniques. It will be shown later that the system performance is not significantly degraded when the nonlinear system is substituted for its linear equivalent.

2.2.4 Strip dynamics. The strip dynamics are modelled as a combination of pure time delay and a simple lag. This allows for the time taken for the strip to travel the 2.9 metres from the roll-gap to the shapemeter and for the fact that the stress profile varies between the roll-gap and the shapemeter. Thus for each zone of the strip, the above dynamics are represented by the second order

transfer function:

$$T_s(s) = \frac{(1-s\frac{\tau}{2})}{(1+s\frac{\tau}{2})(1+s\tau_1)} \qquad (9)$$

where $\tau = D/v$ and $\tau_1 = D_1/v$, being the strip speed in m/s, D the distance from the roll-gap to the shapemeter (2.91m) and $D_1$ the distance between the roll-gap and coiler (5.32m). Equation (9) includes a Pade approximation to the time delay.

2.2.5 Shapemeter. A number of independent first-order transfer functions are used as a representation for the shapemeter; the transfer functions being the same in each zone and strip speed dependent:

$$T_o(s) = \frac{1}{(1+s\tau_o)} \qquad (10)$$

| Strip speed | → 2 m/s | 2 m/s → 5 m/s | 5 m/s → 15 m/s |
|---|---|---|---|
| $\tau_o$ | 1.43 | 0.74 | 0.3 |

2.2.6 Input strip shape. This is the disturbance input into the plant and represents the residual shape profile contained in the strip due to hot rolling and previous cold rolling passes. It is modelled as a constant profile with sinusoidal variations in each of the eight points which describe the profile.

## 2.3 Plant Transfer Function Matrix

The plant transfer function matrix may be written as:

$$\omega(s) = \frac{\gamma(s)}{\sigma(s)} G_M \qquad (11)$$

and for low, medium and high speed ranges $\gamma(s)/\sigma(s)$ has the respective forms:

$$\frac{\gamma(s)}{\sigma(s)} = \frac{(1-0.727s)}{(1+0.25s)(1+0.531s)(1+0.727s)(1+2.66s)(1+1.43s)} \qquad (12)$$

$$\frac{\gamma(s)}{\sigma(s)} = \frac{(1-0.291s)}{(1+0.25s)(1+0.531s)(1+0.291s)(1+1.064s)(1+0.74s)} \qquad (13)$$

$$\frac{\gamma(s)}{\sigma(s)} \frac{(1-0.097s)}{(1+0.25s)(1+0.531s)(1+0.097s)(1+0.355s)(1+0.15s)} \qquad (14)$$

## 3. A DETERMINISTIC OPTIMAL CONTROL SOLUTION

A closed loop controller $C_o(s)$ for the output feedback system shown in Fig.2 will be obtained. The step response for the system is important and hence the reference is chosen as $\underline{r}(s) = \underline{k}/s$ where $\underline{k}$ is a constant vector. The initial conditions are assumed to be zero.

The performance criterion to be minimised is defined as follows:

$$J(u) = \int_o^\infty (\langle (Le)(t), Q_1(Le)(t)\rangle_{E_r} + \langle \underline{u}(t), R_1\underline{u}(t)\rangle_{E_M})dt \qquad (15)$$

where $Q, R > 0$ and L is a linear dynamical operator.

## 3.1 Closed Loop Optimal Deterministic Controller

If the gradient function is defined as $\underline{g} = \frac{1}{2}\partial J/\partial \underline{u}$, and the error, $\underline{e}$, in the cost function is replaced by $\underline{r} - W\underline{u}$, the transformed gradient may be obtained as:

$$\hat{\underline{g}}(s) = [W^T(-s)L^T(-s)Q_1L(s)W(s)+R_1]\underline{u}(s) - W^T(-s)L^T(-s)Q_1\underline{r}(s) \qquad (16)$$

The matrix $[W^T(-s)L^T(-s)Q_1L(s)W(s)+R_1]$ can be spectrally factored giving:

$$Y^T(-s)Y(s) = [W^T(-s)L^T(-s)Q_1L(s)W(s)+R_1] \qquad (17)$$

and from

$$[Y^T(-s)]^{-1}\hat{\underline{g}}(s) + \{[Y^T(-s)]^{-1}W^T(-s)L^T(-s)Q_1\underline{r}(s)\}_- = Y(s)\hat{\underline{u}}(s) - \{[Y^T(-s)]^{-1}W^T(-s)L^T(-s)Q_1\underline{r}(s)\}_+ \qquad (18)$$

where $\{\cdot\}_+ \Rightarrow$ analytic in the closed right half plane and $\{\cdot\}_- \Rightarrow$ analytic in the closed left half plane.
Equation (18) implies that both the LHS and RHS are zero giving:

$$\{[Y^T(-s)]^{-1}W^T(-s)L^T(-s)Q_1\underline{r}(s)\}_+ = Y(s)\hat{\underline{u}}(s) \qquad (19)$$

Write,

$$P(s)\underline{r}(s) = Y(s)\hat{\underline{u}}(s) \qquad (20)$$

where P(s) is a transfer function matrix, and

$$\underline{u}(s) = [Y(s)]^{-1}P(s)\underline{r}(s) = F_o(s)\underline{r}(s)$$

where $F_o(s)$ is the required open loop controller matrix. Therefore the required closed loop controller matrix is given by:

$$C_o(s) = F_o(s)[I - W(s)F_o(s)]^{-1} \qquad (21)$$

Substituting for the plant matrix $W(s) = G_M\,\gamma(s)/\sigma(s)$ and taking $L(s) = I$ and working back through equations (19) (20) and (21) and noting that

$$Y^T(-s)Y(s) = W^T(-s)Q_1W(s)+R_1 = \frac{N^T(-s)N(s)}{\sigma(-s)\sigma(s)} \qquad (22)$$

where N(s) is a polynomial matrix, $C_o(s)$ can be obtained as:

$$C_o(s) = [G_M^{-1}Q_1^{-1}G_M^{-T}N(o)^TN(s) - \gamma(s)I_M]^{-1}G_M^{-1}\sigma(s) \qquad (23)$$

## 3.2 Provision of Integral Action

Alternatively, if L(s) is chosen to be $I_M/s$ to achieve zero steady state error, $C_o(s)$ becomes:

$$C_o(s) = N(s)^{-1}(M_1+sM_2)(I_m - \gamma(s)N(s)^{-1}(M_1+sM_2))^{-1}G_M^{-1}\sigma(s) \qquad (24)$$

where $M_1 = Q^{\frac{1}{2}}G_M$

$$N^T(-s)N(s) = G_M^TQ_1G_M\gamma(-s)\gamma(s) - s^2R_1\sigma(-s)\sigma(s)$$

and $M_2 = \lim_{s\to o}(N(s) - Q_1^{\frac{1}{2}}G_m\gamma(s))/s$

In the limit as $s\to o$, $C_o(s)\to\infty$, signifying the presence of integral action.

## 3.3 Problem Reduction by Diagonalisation

If the error weighting matrix $Q_1$ is chosen to be $Q_1 \triangleq G_M^{-T}Q_oG_M^{-1}$ and $Q_o$, $R_1$ are diagonal matrices then from (23):

$$C_o(s) = [Q_o^{-1}(Q_o+R_1)^{\frac{1}{2}}N(s) - \gamma(s)I_M]^{-1}G_M^{-1}\sigma(s) \qquad (25)$$

The above choices for $Q_1$ and $R_1$ diagonalise the controller for the integral control case. This choice for $Q_1$ accords with weighting the transformed shape error profile. This signal represents the error profile which the outputs of the As-U-Roll actuators must correct and it is important to limit these errors because of the constraints on actuator movement.

The solution presented in (25) may be justified physically by observing that the plant pole polynomial is cancelled by the controller and $G_M^{-1}$ in the controller results in m effective single-loop systems. If we assume that the normalised zero frequency gain in each loop is

unity then $C_o(s)$ reduces to the scalar transfer function given by:

$$C_o(s) = \frac{q\sigma(s)}{(n(s)(q+r)^{\frac{1}{2}} - q\gamma(s))} \quad (26)$$

where n(s) satisfies

$$n(s)n(-s) = q\gamma(s)\gamma(-s) + r\sigma(s)\sigma(-s) \quad (27)$$

and $\gamma(o) = \sigma(o) = 1$ and $C_o(o) = q/r$.

### 3.4 Diagonalisation with Integral Control

If the cost function includes the term L(s) = I/s then integral control results and the closed-loop controller is obtained as follows:

$$Y^T(-s)Y(s) = (q\tilde{\gamma}\gamma - s^2 r\tilde{\sigma}\sigma)/(-s^2\tilde{\sigma}\sigma) = \tilde{n}n/-s^2\tilde{\sigma}\sigma) \quad (28)$$

thence

$$Y(s) = n(s)/s\sigma(s) \quad (29)$$

$$F_o(s) = \frac{\sigma(s)}{n(s)}(m_1 + sm_2) \quad (30)$$

where $n(o) = q^{\frac{1}{2}}$, $m_1 = \lim_{s\to o}(n(s) - q^{\frac{1}{2}}\gamma(s))/s$

and

$$n(s)n(-s) = q\gamma(s)\gamma(-s)rs^2\sigma(s)\sigma(-s) \quad (31)$$

giving:

$$C_o(s) = \frac{\sigma(s)(m_1+sm_2)}{(n(s)-\gamma(s)(m_1+sm_2))} \quad (32)$$

The most sensible choice of controller would seem to be that given in either (26) or (32) but these controllers may not be the least sensitive to errors in the modelling of the $G_M$ matrix. If squaring down matrices are not used the matrix will not be full rank in which case the controller must be calculated using either (23) or (24).

*Note:* A more complete derivation of (21) can be obtained in Grimble, 1977[7].

## 4. RESULTS

### 4.1 Single Loop Response

Calculation of the single-loop controller given in (26) for the medium speed plant in (13) with $q_{ii} = 100$ and $r_{ii} = 1$ (giving a steady state error of less than 1%) yields:

$$C_o(s) = \frac{0.0304s^5+0.3531s^4+1.532s^3+3.081s^2+2.876s+1.0}{3.055\times10^{-3}s^5+0.04218s^4+0.239s^3+0.727s^2+1.546s+0.01} \quad (33)$$

For this choice of q and r, a pole occurs at s = -0.00635 which gives a response similar to the integral action controller (32).

The system unit step response using the above controller is shown in Fig.4.

### 4.2 Shape Control

With an input shape profile as shown in Fig.5, the variation in output shape profile with time is as shown in Fig. 6.

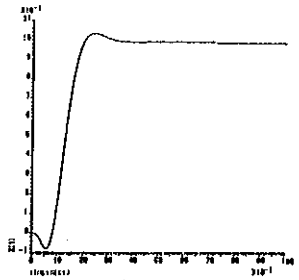

Figure 4: Single Loop Unit Step Response

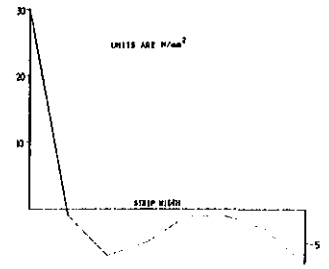

Figure 5: Incoming Strip Shape Profile

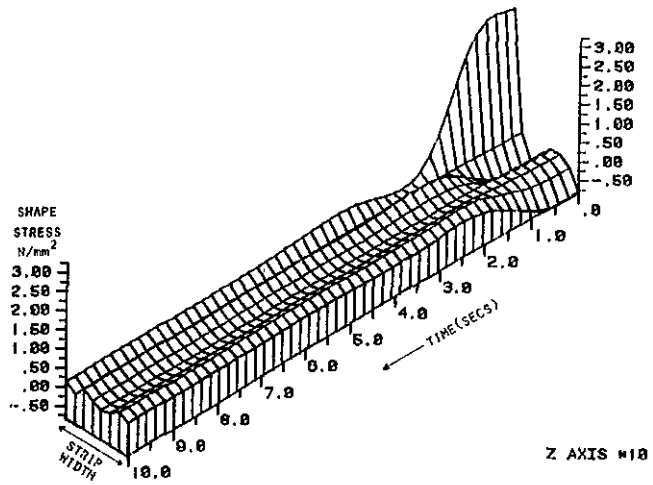


Figure 6: Strip Shape Variations for Linear System

.2.1 Shape control with nonlinearities. When the nonlinear actuator transfer function is substituted for the linear approximation upon which the design was based, the following variation in output shape profile is obtained:

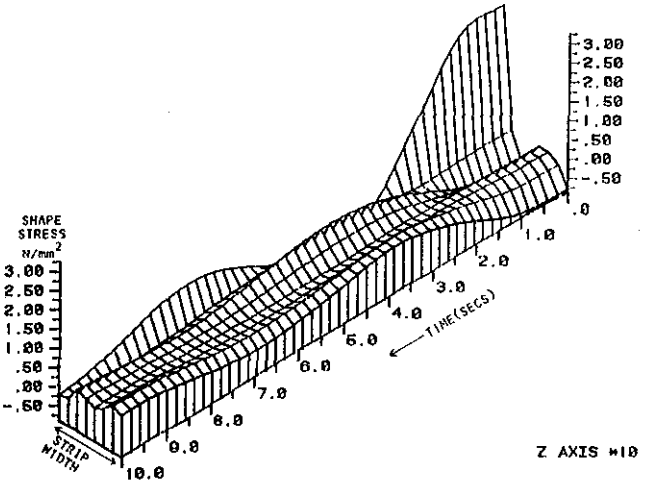


Figure 7: Strip Shape Variations for Nonlinear System

4.2.2 Shape control with mismatched precompensator. Due to modelling errors in $G_M$ and the fact that $G_M$ varies from pass to pass and schedule to schedule, it is necessary to observe the effect of a mismatch in the diagonalising precompensator. Fig.8 shows the effect of using a precompensator calculated for a different schedule.

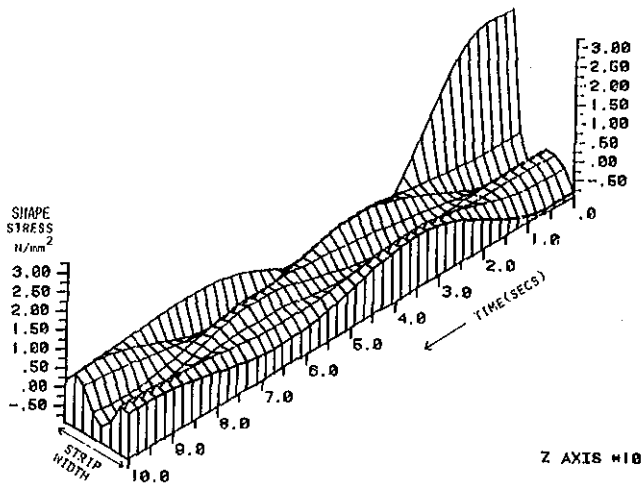


Figure 8: Strip Shape Variations for Nonlinear System with Mismatch

## 5. DISCUSSION OF RESULTS

The optimal system is two or three times faster than was obtained for the same overshoot using PI control (medium speed). Fig.9 shows the time response using a typical first order controller where

$$C_o(s) = \frac{0.4(s + 0.7)}{s + 0.001}$$

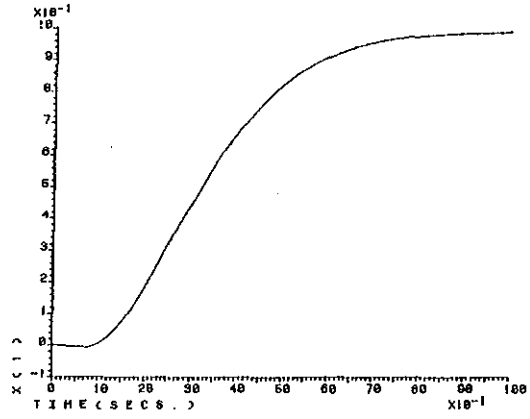


Figure 9: Unit Time Response Using 1st Order Controller

Note that there is a 3 second (approx) time difference to 100% between figures 4 and 9 and this is equivalent to 15 metres of steel strip.

Mismatch between the actual $G_M$ and that used for the controller calculations results in some limited interaction between the various loops but is effect is not significant as can be seen from Fig.8.

It is also seen that the linear design works quite well with the nonlinear actuators.

## 6. CONCLUSIONS

The shape control problem has been reduced to a number of SISO designs. The controller has this simple form when the error weighting matrix $Q_1$ has the specific form

$$Q_1 = G_M^{-T} Q_o G_M^{-1}.$$

The shape error term in the cost function in this case is transformed by $G_M^{-1}\underline{e}(t)$ before being costed. The diagonal matrix $Q_o$ therefore penalises shape errors referred to the mill inputs. This result has some value since adjacent As-U-Roll actuators can only be changed by a limited amount. Thus in choosing $Q_o$ and $R_1$, the relative importance of shape error and control action at a particular actuator is considered.

The optimal control solution indicates that the cancellation of the stable plant poles is required. This have some merit becuase the plant has a number of break-points in the same frequency range and using classical design methods these must be cancelled to achieve reasonable gains and relative stability.

ACKNOWLEDGEMENTS

We are grateful for the support of GEC Electrical Projects Limited, Rugby and the British Steel Corporation, Sheffield. We are grateful for the contributions to the project by Mr. K. Dutton of BSC and for the help of Mr. A. Kidd of GEC.

## REFERENCES

1. Bryant, G.F. 'Automation of tandem mills', The Iron and Steel Institute, 1973.

2. Grimble, M.J., 'Shape control for rolled strip', CME November 1975, pp 91-93.

3. Sivilotti, O.G., Davies, W.E., Henze, M. and Dahle, O, Asea-Alcan AFC Systems for Cold Rolling Flat Strip, Iron and Steel Engineer, June 1973, pp 83-90.

4. Sanatini, B. and Yeomans, K.A., 'An algebra of strip shape and its application to mill scheduling', Journal of the Iron and Steel Institute, December 1968, pp 1207-1217.

5. Grimble, M.J. and Fotakis, J., 'The design of strip shape control systems for Sendzimir mills', IEEE Transactins on Automatic Control, Vol. AC-27, No. 3, June 1982.

6. Gunawardene, C.W.D.M., Grimble, M.J. and Thomson, A., 'A static model for a Sendzimir cad rolling mill', Metals Technology, 1980.

7. Grimble, M.J., 'Design of optimal machine-control systems', Proc IEE, Vol.124, No.9, September 1977, pp 821-827.